11. Cesare, P. & McNaughton, P. A novel heat-activated current in nociceptive neurons and its sensitization by bradykinin. *Proc. Natl Acad. Sci. USA* **93,** 15435–15439 (1996).
12. Nagy, I. & Rang, H. P. Similarities and differences between the responses of rat sensory neurons to noxious heat and capsaicin. *J. Neurosci.* **19,** 10647–10655 (1999).
13. Nagy, J. I. & Kooy, D. van der. Effects of neonatal capsaicin treatment on nociceptive thresholds in the rat. *J. Neurosci.* **3,** 1145–1150 (1983).
14. Caterina, M. J., Rosen, T. A., Tominaga, M., Brake, A. J. & Julius, D. A capsaicin-receptor homologue with a high threshold for noxious heat. *Nature* **398,** 436–441 (1999).
15. Hargreaves, K., Dubner, R., Brown, F., Flores, C. & Joris, J. A new and sensitive method for measuring thermal nociception in cutaneous hyperalgesia. *Pain* **32,** 77–88 (1988).
16. Kwak, J. Y., Jung, J. Y., Hwang, S. W., Lee, W. T. & Oh, U. A capsaicin-receptor antagonist, capsazepine, reduces inflammation-induced hyperalgesic responses in the rat: evidence for an endogenous capsaicin-like substance. *Neuroscience* **86,** 619–626 (1998).
17. Sasamura, T., Sasaki, M., Tohda, C. & Kuraishi, Y. Existence of capsaicin-sensitive glutamatergic terminals in rat hypothalamus. *Neuroreport* **9,** 2045–2048 (1998).
18. Rogers, D. C. *et al.* 'SHIRPA'—a comprehensive behavioural and functional analysis of mouse phenotype. *Mamm. Genome* **8,** 711–713 (1997).
19. Yagi, T. *et al.* A novel selection for homologous recombinants using diptheria toxin A frgament gene. *Anal. Biochem.* **214,** 77–86 (1993).
20. Torres, R. M. & Kuhn, R. *Laboratory Protocols for Conditional Gene Targeting.* (Oxford Univ. Press, Oxford, 1997).
21. Hooper, M., Hardy, K., Handyside, A., Hunter, S. & Monk, M. HPRT-deficient (Lesch-Nyhan) mouse embryos derived from germline colonization by cultured cells. *Nature* **326,** 292–295 (1987).
22. Rogers, D. C. *et al.* Use of SHIRPA and discriminant analysis to characterise marked differences in the behavioural phenotype of six inbred mouse strains. *Behav. Brain Res.* **105,** 207–217 (1999).
23. Miliken, G. A. & Johnson, D. E. in *Analysis of Messy Data* 29–45 (Chapman & Hall, London, 1992).

Supplementary information is available on *Nature*'s World-Wide Web site (http://www.nature.com) or as paper copy from the London editorial office of *Nature*.

Acknowledgements

The authors would like to acknowledge P. Hayes, J. Nation, S. Pickering and C. David for technical assistance, and S. Rastan, F. Walsh, M. Geppert and D. Simmons for valuable critique.

Correspondence or requests for materials should be addressed to J.B.D. (e-mail: John_B_Davis@sbphrd.com).

Glutamatergic synapses on oligodendrocyte precursor cells in the hippocampus

Dwight E. Bergles*, J. David B. Roberts†, Peter Somogyi† & Craig E. Jahr*

** Vollum Institute, L474, Oregon Health Sciences University, Portland, Oregon 97201, USA*
† MRC Anatomical Neuropharmacology Unit, Department of Pharmacology, University of Oxford, Oxford OX1 3TH, UK

Fast excitatory neurotransmission in the central nervous system occurs at specialized synaptic junctions between neurons, where a high concentration of glutamate directly activates receptor channels. Low-affinity AMPA (α-amino-3-hydroxy-5-methyl isoxazole propionic acid) and kainate glutamate receptors are also expressed by some glial cells[1], including oligodendrocyte precursor cells (OPCs). However, the conditions that result in activation of glutamate receptors on these non-neuronal cells are not known. Here we report that stimulation of excitatory axons in the hippocampus elicits inward currents in OPCs that are mediated by AMPA receptors. The quantal nature of these responses and their rapid kinetics indicate that they are produced by the exocytosis of vesicles filled with glutamate directly opposite these receptors. Some of these AMPA receptors are permeable to calcium ions, providing a link between axonal activity and internal calcium levels in OPCs. Electron microscopic analysis revealed that vesicle-filled axon terminals make synaptic junctions with the processes of OPCs in both the young and adult hippocampus. These results demonstrate the existence of a rapid signalling pathway from pyramidal neurons to OPCs in the mammalian hippocampus that is mediated by excitatory, glutamatergic synapses.

Oligodendrocytes in the mammalian central nervous system develop from a population of precursor cells during late gestational and early postnatal life[2], providing the insulating sheaths of myelin necessary for rapid conduction of action potentials along axons. These precursors or OPCs were identified anatomically as smooth protoplasmic astrocytes based on their unique stellate morphology[3], and their properties have been studied both in culture (termed O-2A cells)[4–6] and in acutely isolated tissue (termed glial precursors or complex cells)[1,7]. Glutamate receptor activation in these cells inhibits their proliferation and maturation into oligodendrocytes[8], and prolonged exposure to glutamate causes excitotoxic degeneration[9]. Despite the potential importance of this pathway in the development and regeneration of myelin, it is not known how these receptors are activated *in vivo*. Glutamate has been shown to reach other glial cells by diffusion from nearby synaptic clefts following vesicular release[10], or by reverse transport along axons[11].

To determine how glutamate reaches AMPA receptors on OPCs, we made whole-cell patch-clamp recordings from OPCs in the hippocampus and measured their response to stimulation of afferent excitatory axons. OPCs located in the stratum radiatum region of area CA1 exhibited small Na^+ currents, large A-type and delayed rectifier K^+ currents, and did not fire action potentials (Fig. 1a) (n = 28). Electrical stimulation in stratum radiatum elicited inward currents in OPCs that had rapid kinetics (Fig. 1b). Cells with these properties had a stellate morphology, with thin, highly branched processes that extended from a small cell body (Fig. 1c). They were identified as OPCs by their immunoreactivity to NG2 (Fig. 1d, e, n = 10/10), a proteoglycan that is only expressed by OPCs in this region[12]. These NG2-positive cells were immunonegative for glial fibrillary acidic protein (n = 3/3), while astrocytes recorded from under similar conditions were immunopositive (n = 8/8 groups of cells).

Paired stimuli produced currents in OPCs that were larger (P2/P1 = 1.7 ± 0.1, n = 16) and exhibited fewer apparent failures following the second stimulus (Fig. 2a), similar to paired-pulse facilitation of excitatory postsynaptic currents (EPSCs) in CA1

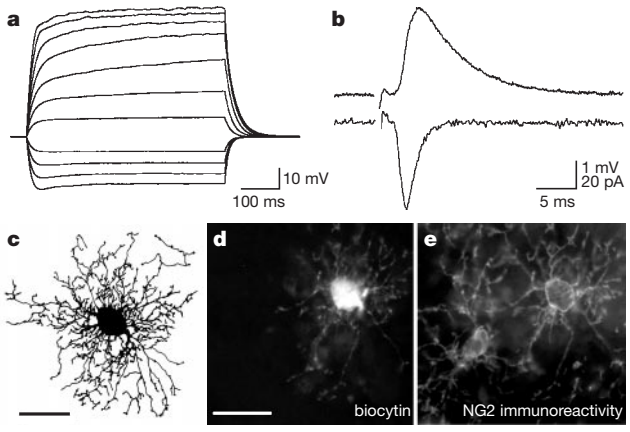

Figure 1 Synaptic responses from identified OPCs in hippocampal slices. **a**, Current-clamp recording of membrane responses to current injection (–80 to 140 pA; step size, 20 pA). **b**, Evoked responses to Schaffer collateral/commissural fibre stimulation, recorded in voltage-clamp (holding potential, –90 mV; lower trace) and current-clamp (membrane potential = –90 mV; upper trace). Traces are averages of 15 consecutive responses recorded from the same cell. Stimulus: 30 μA, 100 μs. **c**, Reconstruction of a biocytin-filled OPC. **d**, Micrograph of the same OPC as in **d**, visualized by AMCA-conjugated streptavidin. **e**, NG2-immunoreactivity of same region of the slice as shown in **d**. Scale bars for **c** and **d,** 20 μm; **d** and **e** are at the same magnification.

pyramidal neurons. These currents were blocked by the competitive AMPA/kainate receptor antagonist 2,3-dihydroxy-6-nitro-7-sulphamoyl-benzo(F)quinoxaline (NBQX, 5 μM; $n = 28$) (Fig. 2a), and strongly inhibited (>95%) by 1-(4-aminophenyl)-4-methyl-7,8-methylenedioxy-5H-2,3-benzodiazepine hydrochloride (GYKI 52466, 50 μM), a non-competitive AMPA receptor antagonist ($n = 4$). Cyclothiazide (CTZ, 100 μM), which potentiates currents mediated by AMPA, but not kainate receptors[13], increased the amplitude (282 ± 41%, $n = 12$) and slowed the time constant of decay ($\tau_{control} = 1.21 \pm 0.09$ ms, $\tau_{CTZ} = 3.76 \pm 0.14$ ms, $n = 12$) of evoked responses. The sensitivity of these currents to both CTZ and GYKI 52466 indicates that they are mediated by AMPA receptors. Evoked currents in OPCs were also reversibly blocked by Cd^{2+} (30 μM), indicating that they are dependent on Ca^{2+} release mechanisms and are not produced by reverse transport of glutamate[11,14] (Fig. 2b). EPSCs in CA1 pyramidal neurons are markedly enhanced by antagonists of A_1 adenosine receptors, such as 8-cyclopentyltheophylline (CPT), resulting from the relief of presynaptic inhibition by ambient adenosine[15]. The amplitudes of OPC responses were also increased (252 ± 41%, $n = 6$) by CPT (1 μM), indicating that the release of glutamate onto OPCs is under similar inhibitory control (Fig. 2b).

AMPA receptors lacking the edited GluRB (GluR2) subunit are permeable to Ca^{2+} and exhibit rectifying current–voltage (I–V) relationships due to channel block by internal polyamines[16]. To determine whether AMPA receptors activated in OPCs with axonal stimulation were permeable to Ca^{2+}, we examined the I–V relationship of evoked responses. Slight inward rectification was observed under control conditions that was enhanced by including spermine (25 μM) in the internal solution (Fig. 2c), indicating that Ca^{2+}-permeable AMPA receptors contribute to the evoked synaptic currents. In addition, these currents were inhibited by Joro spider toxin (5 μM, $n = 4$), a selective antagonist of Ca^{2+}-permeable AMPA/kainate receptors[13]. These results indicate that activity of glutamatergic afferents is linked to Ca^{2+} entry into OPCs.

Axons from CA3 pyramidal neurons form synapses with dendritic spines of CA1 pyramidal neurons in the stratum radiatum region[16]. To test whether excitatory inputs to OPCs also arise from CA3 pyramidal neurons, we recorded from OPCs in stratum radiatum of area CA1 and focally applied L-glutamate (200 μM) onto the cell body layer of area CA3 (Fig. 2d). In several cells (3/11), glutamate application elicited brief bursts of inward currents in

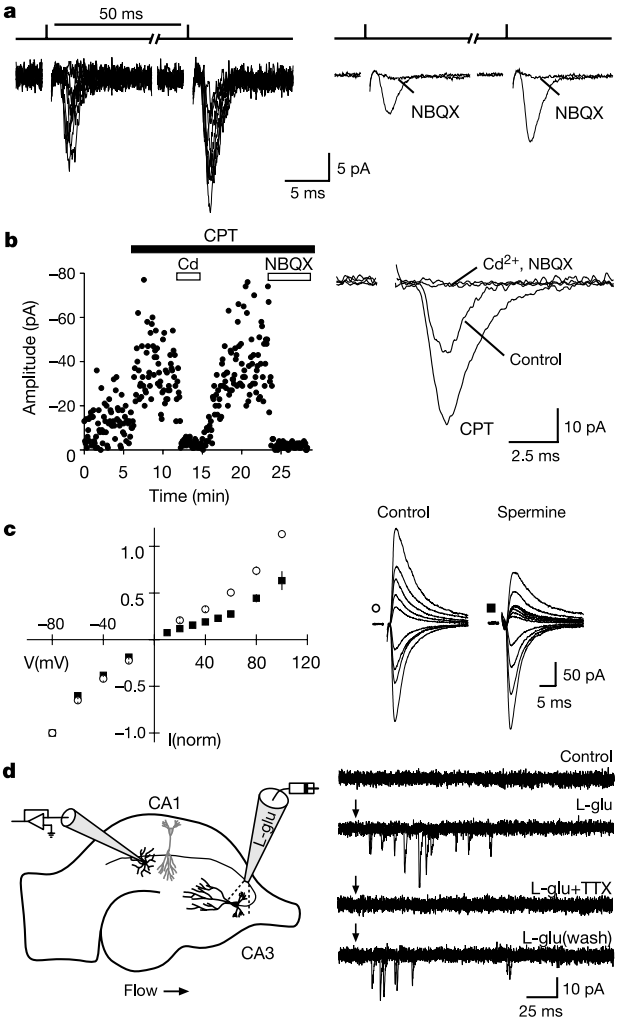

Figure 2 Properties of excitatory responses in OPCs. **a**, Facilitation of evoked responses by paired stimuli. Evoked inward currents were blocked by NBQX (5 μM). Traces at right are averages of 15 consecutive responses. **b**, Plot of peak amplitudes of evoked responses that were increased by CPT (1 μM) and blocked by cadmium 'Cd' ($CdCl_2$, 30 μM) or NBQX (5 μM). Traces at right are averages of 15 consecutive responses. **c**, I–V relationship of evoked responses under control conditions (open circles), or with spermine (25 μM) in the intracellular solution (filled squares). ACSF contained CTZ (100 μM) and CPT (1 μM). Traces at right are averages of 10 consecutive responses recorded at –80 to 100 mV (step size, 20 mV). **d**, Puffer application of L-glutamate (200 μM, 50 ms; down arrow) onto CA3 pyramidal neurons (diagram at left) elicited bursts of inward currents in OPCs that were blocked by TTX (1 μM). Traces at right are overlays of 5 consecutive sweeps.

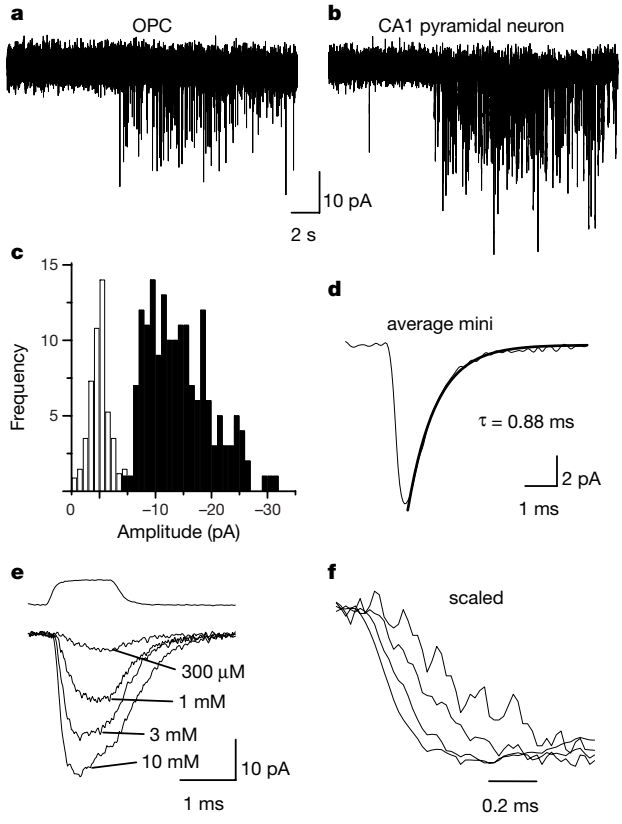

Figure 3 Quantal EPSCs in OPCs are elicited by a brief, high concentration of glutamate. Pardaxin (2 μM) triggered bursts of mEPSCs in OPCs (**a**) and CA1 pyramidal neurons (**b**). **c**, Amplitude distribution of mEPSCs recorded from an OPC. **d**, Average time course of 169 mEPSCs recorded from an OPC. Thick line is a single exponential fit to the decay. **a**, **c**, **d** are from the same cell. **e**, Concentration dependence of the kinetics of AMPA/kainate receptors in outside-out patches from OPCs. Traces are averages of 30 consecutive responses. **f**, The rising phase of responses in **e** shown scaled to the peak of the response to 10 mM L-glutamate.

OPCs (Fig. 2d). These glutamate-evoked currents were blocked by the Na^+ channel antagonist, tetrodotoxin (TTX, 1 μM), indicating that they were dependent on propagation of action potentials from CA3. Because the only glutamatergic neurons located in the CA3 region are pyramidal neurons[16], these results suggest that Schaffer collateral axons of CA3 pyramidal neurons provide excitatory input to both OPCs and CA1 pyramidal neurons.

Spontaneous fusion of transmitter-filled vesicles occurs at individual excitatory synapses in the absence of action potentials, resulting in miniature EPSCs (mEPSCs)[17]. Similar miniature AMPA receptor-mediated currents were observed in OPCs at a very low frequency (<0.01 Hz). Brief application of the presynaptic neurotoxin pardaxin (2 μM), which enhances the frequency of vesicular release from nerve terminals[18], caused the appearance of high-frequency bursts of mEPSCs in both OPCs (n = 11 cells) (Fig. 3a) and CA1 pyramidal neurons (n = 6 cells) (Fig. 3b); similar bursts were induced in OPCs by α-latrotoxin (2 nM, n = 4 cells). The amplitudes of mEPSCs recorded from OPCs were highly variable

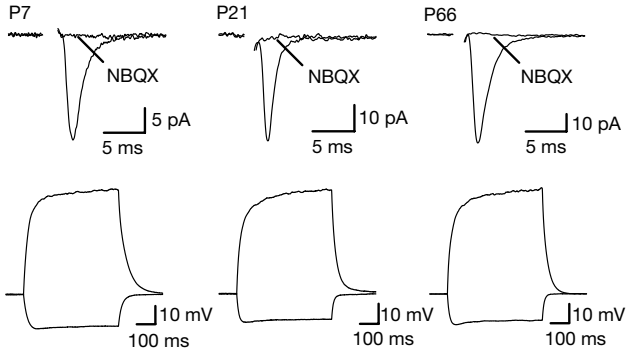

Figure 4 Excitatory synaptic responses were evoked in OPCs from both young and adult animals. EPSCs from OPCs in hippocampal slices prepared from different age animals were blocked by NBQX (5 μM). Stimulus intensity was 20–30 μA, 100 μs. ACSF contained CPT (1 μM). Lower traces show membrane responses of OPCs from these age animals to current injection (–60 and 120 pA).

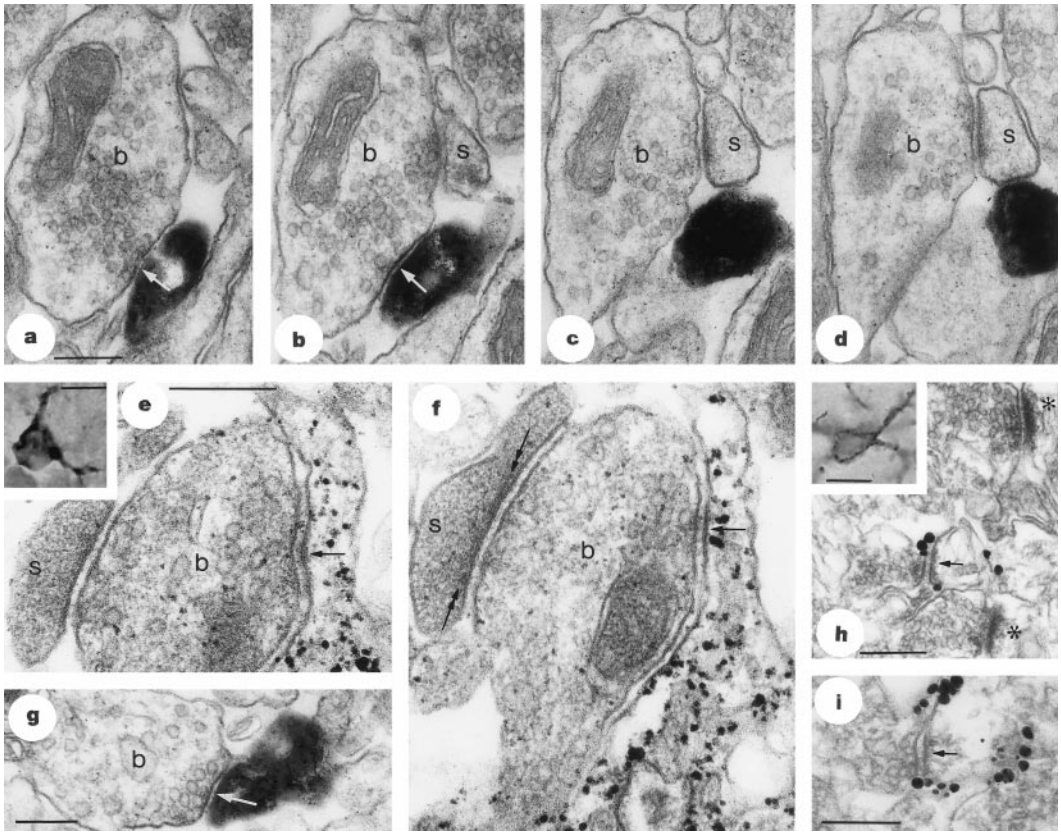

Figure 5 Electron micrographs of the synaptic relationships of OPCs. **a–d**, Serial sections of a process (black, peroxidase reaction) from a physiologically identified, biocytin labelled OPC receiving a synapse (arrow) from a bouton (b) that also gives a synapse to a dendritic spine (s). The OPC process approaches the spine postsynaptic density to within ~110 nm (**c**). **e**, **f**, Silver-intensified gold reaction of an OPC (inset, light micrograph) process reveals the thinner postsynaptic membrane specialization (arrows) as compared with the postsynaptic density (between double arrows) of a spine (s) innervated by the same bouton (b). **g**, Another bouton (b) made a synapse (arrow) only with an OPC process. **h**, **i**, NG2-immunopositive OPC (inset) visualized with an antibody to an extracellular epitope, resulting in silver/gold particles (electron-opaque dots) surrounding OPC processes in stratum radiatum of adult rat. The postsynaptic membrane specialization is thinner than that of neighbouring synapses on dendritic spines (asterisks). Scale bars for **a**–**i**, 0.2 μm; scale bars in insets, 10 μm.

(coefficient of variance, 35 ± 4%; mean amplitude, 15 ± 3 pA; n = 11 cells), and did not conform to a normal distribution (Fig. 3c), similar to mEPSCs recorded from neurons in many brain regions[17]. The small size of the mEPSCs and the indication that they arise from Schaffer collateral fibres that have a low release probability[19], suggests that approximately 60 inputs would have to be stimulated to elicit a −100 pA synaptic current in an OPC. The average time course of these mEPSCs was very fast, rising in 259 ± 15 μs (20–80%; range, 179–335 μs; n = 11 cells) and decaying with a time constant of 983 ± 58 μs (range, 700–1,250 μs; n = 11 cells) (Fig. 3d).

To estimate the amount of glutamate necessary to produce AMPA receptor-mediated mEPSCs in OPCs, we measured the concentration-dependence of the kinetics of these receptors in isolation, by applying different concentrations of glutamate to outside-out patches removed from OPCs. A concentration of 3 mM L-glutamate was necessary to produce currents with a rise time similar to the mEPSCs (10 mM, 180 ± 29 μs; 3 mM, 286 ± 48 μs; 1 mM, 397 ± 56 μs; 300 μM, 1,184 ± 191 μs; n = 5) (Fig. 3e, f). These data and the less than threefold increase in OPC synaptic responses produced by CTZ[20] indicates that the mEPSCs are not produced by a low concentration glutamate diffusing out of nearby neuronal synapses[10]. These results suggest that numerous excitatory synapses are formed on OPCs.

The link between glutamate receptor activation and OPC differentiation[8] raised the possibility that these excitatory synapses are present only during early development. However, OPCs with similar electrophysiological properties were identified in slices prepared from both young (postnatal day 7, P7, n = 4; P21, n = 10), and mature animals (P66, n = 5) (Fig. 4), consistent with previous immunocytochemical results indicating that these cells are abundant in both developing and adult brain[7,12], and OPCs from all ages received similar excitatory synaptic input (Fig. 4).

Biocytin loading of OPCs made it possible to identify the relationships of their processes to neuronal synaptic membranes. Electron microscopy revealed presynaptic transmitter release sites that were identified on the basis of clustering of synaptic vesicles to a membrane region exhibiting electron-opaque clumps of granular material (presynaptic dense projections) (Fig. 5). In the first type of synaptic relationship, OPC processes were directly apposed to presynaptic release sites as seen for cells visualized by peroxidase (n = 2) (Fig. 5a–d, g) or gold/silver (n = 2) methods (Fig. 5e, f). Axonal and glial membranes were rigidly apposed in the synaptic junction (49 synapses, 7–19 per cell, 44 completely serially sectioned), and contained electron-opaque cleft material and an intracleft disk. Four presynaptic terminals also made another synaptic junction with a nearby dendritic spine in the sectioned zone (Fig. 5b–g), confirming the common origin of innervating afferents from CA3. The postsynaptic membrane specialization of the glial membrane was much thinner than that of nearby type 1 synapses on spines (Fig. 5e, f, h, i), and most synaptic junctions received by OPCs were small (largest extent: 0.211 ± 0.077 μm (s.d.); range, 0.062–0.430 μm). The existence of direct synaptic junctions on OPCs suggests that they are responsible for the fast synaptic currents.

In the second type of synaptic relationship, the processes of OPCs were closely aligned to the synaptic cleft of axo-spinous synaptic junctions (Fig. 5c, h). The closest distance between the edge of the postsynaptic density and the OPC process was 74 ± 6 nm (range, 38–136 nm; n = 22; P21 rat). In a series of sections, 22 close alignments to spine synapses and 19 direct synapses were found over 101 μm^2 of OPC membrane, representing about 2.5% of the cell. If cells *in vivo* receive a similar innervation, this suggests that an OPC can receive about 800 direct synapses.

The perisynaptic location of some OPC processes is similar to astrocytic[21] and Bergmann glial cell processes[3]. Glutamate concentration peaks at less than 200 μM at Bergmann glial membranes following release at climbing fibre–Purkinje neuron synapses in the cerebellum[20,22], producing slow AMPA receptor-mediated currents in these cells (20–80% rise time, 1 ms; half decay time, 4.2 ms)[22]. The fast kinetics of OPC responses make it unlikely that they are produced by spillout of glutamate from nearby neuronal synapses. However, the frequent close opposition of OPC processes to axo-spinous synapses raises the possibility that these cells modulate neuronal synaptic transmission.

It is possible that synapses on OPCs are formed only following slice preparation. Immunogold/silver labelling of OPCs *in situ,* for an extracellular epitope of the NG2 proteoglycan in the CA1 hippocampal area from perfusion fixed adult and developing rats, revealed direct synaptic junctions (Fig. 5h, i) (n = 24; 22 completely sectioned) with similar characteristics to those observed in acutely isolated tissue. These results indicate that neuron–OPC synapses are present *in vivo*.

Oligodendrocyte development is regulated by secreted factors[7] and direct cell–cell interactions[23]. This evidence of functional glutamatergic synapses between CA3 pyramidal neurons and CA1 OPCs in the hippocampus during the period of oligodendrocyte maturation[2], provides a pathway for axons to regulate myelination. In the adult central nervous system, OPCs remain numerous in the grey matter where myelination is sparse, and they do not readily proliferate to replace oligodendrocytes that have been damaged or lost through lesions[24] or demyelinating diseases such as multiple sclerosis[25]; this suggests that OPCs are not maintained solely as a reservoir for further oligodendrocyte production. The persistence of a rapid excitatory signalling pathway between axons and OPCs raises the possibility of an additional neuromodulatory role for these cells, possibly through the release of neuroactive substances in response to glutamatergic synaptic input. □

Methods

Slice preparation

Hippocampal slices were prepared from male Sprague–Dawley rats (12–16 d old) in accordance with a protocol approved by the Department of Animal Care at OHSU as described[26], and maintained in a solution consisting of (in mM): 119 NaCl, 2.5 KCl, 2.5 $CaCl_2$, 1.3 $MgCl_2$, 1 NaH_2PO_4, 26.2 $NaHCO_3$ and 11 glucose, saturated with 95% O_2/5% CO_2.

Electrophysiology

Putative OPCs located in stratum radiatum of area CA1 were visualized with infrared/Nomarski videomicroscopy. Cells were selected for recording that had a small round cell body (soma diameter <10 μm), with no large processes extending from it. The internal solution for current-clamp recordings contained (in mM): 130 K-methanesulphonate, 20 HEPES, 10 EGTA, 2 Mg-ATP, 0.4 Na-GTP; pH 7.3, and for voltage-clamp recordings contained (in mM): 100 Cs-methanesulphonate, 20 TEA-Cl, 20 HEPES, 10 EGTA, 1 $MgCl_2$, 4 Mg-ATP, 0.3 Na-GTP; pH 7.3. Holding potentials have been adjusted for a 10-mV junction potential (K-methanesulphonate, 10.2 mV; Cs-methanesulphonate, 10.4 mV). The input resistance of OPCs was 257 ± 28 MΩ (n = 23) with K-methanesulphonate, and >1 GΩ with Cs-methanesulphonate.

Evoked responses were elicited with a constant-current stimulator (Winston Electronics) using bipolar stainless-steel electrodes (tip separation ~ 200 μm) placed in stratum radiatum >50 μm from the cell (stimulus: 10–40 μA, 100 μs). Current-clamp recordings were made using an Axoclamp-2A amplifier (Axon Instruments). Whole-cell evoked currents were recorded at −90 mV using an Axopatch 200A (Axon Instruments), filtered at 2 kHz and sampled at 10–50 kHz. Exogenous L-glutamate (200 μM) was ejected from a patch pipette to stratum pyramidale of area CA3 with pulses of nitrogen (50 ms, 9 p.s.i.) using a picospritzer (General Valve) (Fig. 2d). Spontaneous EPSCs were recorded in the presence of 100 μM picrotoxin and 5 μM SR-95531. Averages of mEPSCs were collected from at least 150 events.

Outside-out patches were removed from cell bodies of OPCs and solutions were rapidly applied, as described[22]. Patch currents were filtered at 5 kHz and sampled at 50 kHz, and were made with the Cs-methanesulphonate-based internal solution. The external solution contained (in mM): 135 NaCl, 2.5 KCl, 2.5 $CaCl_2$, 1.3 $MgCl_2$, 20 HEPES; pH 7.2.

All experiments were performed at 22–24 °C. Data are expressed as mean ± standard error, except where noted. Coefficient of variation was calculated as: (standard deviation/mean) × 100.

Histology

OPCs were filled with biocytin (0.15%). The seal was then destroyed with large negative current pulses (to prevent removal of the cell body with the pipette), and the slice fixed. For electron microscopy, slices were fixed in 3.4% paraformaldehyde, 1.25% glutaraldehyde in

0.1 M phosphate buffer (pH 7.4), freeze-thawed and resectioned at 60 μm. Biocytin was visualized with an avidin-biotinylated-HRP using diaminobenzidine or 1 nm gold-conjugated streptavidin (Nanoprobes). Electron microscopic sections were contrasted with lead citrate. One physiologically identified OPC (P21 rat) was fixed 4 h after slice preparation and evaluated in 23 continuous electron microscopy serial sections, measuring the circumference of its processes. The sections, taken at a level of about half radius of the volume occupied by the cell, covered a depth of 1.61 μm and contained 101 μm^2 of OPC membrane, estimated by multiplying the circumference of processes by the estimated section thickness of 70 nm. Assuming isotropic distribution of the processes (total diameter, 65 μm), about 2.5% of the cell was sampled. Distance from axo-spinous synapses to OPC processes was measured in a straight line for distances less than 150 nm without any intervening cellular elements.

For immunocytochemistry, slices were fixed in 4% paraformaldehyde, 0.05% glutaraldehyde in 0.1 M phosphate buffer (pH 7.4), and resectioned at 60 μm. Antibodies to NG2 were provided by W. B. Stallcup and A. Nishiyama. Anti-rat-NG2 antibodies (ab-NG2EC, 2.8 $\mu g\,ml^{-1}$) were raised in rabbit to a polypeptide representing the extracellular domain (residues 1–2,223)[27]. Monoclonal antibodies (D4, culture-supernatant, diluted 1:50) were raised to rat NG2[28]. Both antibodies label a broad band of relative molecular mass (M_r) of ~400K to 800K on western blots of extracts from rat brain and also from transfected cell lines expressing rat NG2 (A. Nishiyama, personal communication). Guinea pig antibodies to GFAP (1:500) were obtained from Advanced Immunochemicals. Triple fluorescence immunolabelling was performed[29] using AMCA-conjugated streptavidin (Vector Labs) for biocytin, Alexa 488-conjugated anti-rabbit or anti-mouse IgG (Molecular Probes) for NG2, and CY3-conjugated anti-guinea pig IgG (Jackson Labs) for GFAP.

Two adult (>P60) and two developing (P19, 21) male rats (Wistar) were anaesthetized, fixed and immunoreacted with ab-NG2EC (1:500) using silver intensified pre-embedding immunogold reaction (1.4 nm gold conjugated secondary antibody, Nanoprobes) as described[30]. Because these antibodies recognize an extracellular epitope, only the silver intensified immunogold labelling method is suitable for identifying glial processes in the neuropil. No labelling was detected when specific antibodies were replaced with normal serum of the same species or when primary antibody was omitted.

Materials

Pardaxin and α-latrotoxin were purchased from Alamone Labs. All other drugs were purchased from RBI (USA).

Received 17 November 1999; accepted 23 February 2000.

1. Steinhauser, C. & Gallo, V. News on glutamate receptors in glial cells. *Trends Neurosci.* **19,** 339–345 (1996).
2. Miller, R. H. Oligodendrocyte origins. *Trends Neurosci.* **19,** 92–96 (1996).
3. Palay, S. L. & Chan-Palay, V. *Cerebellar Cortex, Cytology and Organization* (Springer, New York, 1974).
4. Raff, M. C., Miller, R. H. & Noble, M. A glial progenitor cell that develops in vitro into an astrocyte or an oligodendrocyte depending on culture medium. *Nature* **303,** 390–396 (1983).
5. Patneau, D. K., Wright, P. W., Winters, C., Mayer, M. L. & Gallo, V. Glial cells of the oligodendrocyte lineage express both kainate- and AMPA-preferring subtypes of glutamate receptor. *Neuron* **12,** 357–371 (1994).
6. Wyllie, D. J., Mathie, A., Symonds, C. J. & Cull-Candy, S. G. Activation of glutamate receptors and glutamate uptake in identified macroglial cells in rat cerebellar cultures. *J. Physiol.(Lond.)* **432,** 235–258 (1991).
7. Barres, B. A. & Raff, M. C. Control of oligodendrocyte number in the developing rat optic nerve. *Neuron* **12,** 935–942 (1994).
8. Gallo, V. *et al*. Oligodendrocyte progenitor cell proliferation and lineage progression are regulated by glutamate receptor-mediated K^+ channel block. *J. Neurosci.* **16,** 2659–2670 (1996).
9. McDonald, J. W., Levine, J. M. & Qu, Y. Multiple classes of the oligodendrocyte lineage are highly vulnerable to excitotoxicity. *Neuroreport* **9,** 2757–2762 (1998).
10. Bergles, D. E., Diamond, J. S. & Jahr, C. E. Clearance of glutamate inside the synapse and beyond. *Curr. Opin. Neurobiol.* **9,** 293–298 (1999).
11. Kriegler, S. & Chiu, S. Y. Calcium signaling of glial cells along mammalian axons. *J. Neurosci.* **13,** 4229–4245 (1993).
12. Ong, W. Y. & Levine, J. M. A light and electron microscopic study of NG2 chondroitin sulfate proteoglycan-positive oligodendrocyte precursor cells in the normal and kainate-lesioned rat hippocampus. *Neurosci.* **92,** 83–95 (1999).
13. Dingledine, R., Borges, K., Bowie, D. & Traynelis, S. F. The glutamate receptor ion channels. *Pharmacol. Rev.* **51,** 7–61 (1999).
14. Zerangue, N. & Kavanaugh, M. P. Flux coupling in a neuronal glutamate transporter. *Nature* **383,** 634–637 (1996).
15. Dunwiddie, T. V. The physiological role of adenosine in the central nervous system. *Int. Rev. Neurobiol.* **27,** 63–139 (1985).
16. Amaral, D. G. & Witter, M. P. The three dimensional organization of the hippocampal formation: a review of anatomical data. *Neurosci.* **31,** 571–591 (1989).
17. Lisman, J. E. & Harris, K. M. Quantal analysis and synaptic anatomy - integrating two views of hippocampal plasticity. *Trends Neurosci.* **16,** 141–147 (1993).
18. Renner, P., Caratsch, C. G., Waser, P. G., Lazarovici, P. & Primor, N. Presynaptic effects of the pardaxins, polypeptides isolated from the gland secretion of the flatfish Pardachirus Marmoratus. *Neurosci.* **23,** 319–325 (1987).
19. Hessler, N. A., Shirke, A. M. & Malinow, R. The probability of transmitter release at a mammalian central synapse. *Nature* **366,** 569–572 (1993).
20. Dzubay, J. A. & Jahr, C. E. The concentration of synaptically released glutamate outside of the climbing fiber-purkinje cell synaptic cleft. *J. Neurosci.* **19,** 5265–5274 (1999).
21. Ventura, R. & Harris, K. M. Three-dimensional relationships between hippocampal synapses and astrocytes. *J. Neurosci.* **19,** 6897–6906 (1999).
22. Bergles, D. E., Dzubay, J. A. & Jahr, C. E. Glutamate transporter currents in bergmann glial cells follow the time course of extrasynaptic glutamate. *Proc. Natl Acad. Sci. USA* **94,** 14821–14825 (1997).
23. Wang, S. *et al*. Notch receptor activation inhibits oligodendrocyte differentiation. *Neuron* **21,** 63–75 (1998).
24. Keirstead, H. S., Levine, J. M. & Blakemore, W. F. Response of the oligodendrocyte progenitor cell population (defined by NG2 labelling) to demyelination of the adult spinal cord. *Glia* **22,** 161–170 (1998).
25. Wolswijk, G. Chronic stage multiple sclerosis lesions contain a relatively quiescent population of oligodendrocyte precursor cells. *J. Neurosci.* **18,** 601–609 (1998).
26. Bergles, D. E. & Jahr, C. E. Synaptic activation of glutamate transporters in hippocampal astrocytes. *Neuron* **19,** 1297–1308 (1997).
27. Tillet, E., Ruggiero, F., Nishiyama, A. & Stallcup, W. B. The membrane-spanning proteoglycan NG2 binds to collagens V and VI through the central nonglobular domain of its core protein. *J. Biol. Chem.* **272,** 10769–10776 (1997).
28. Stallcup, W. B., Dahlin, K. & Healy, P. Interaction of the NG2 chondroitin sulfate proteoglycan with type VI collagen. *J. Cell Biol.* **111,** 3177–3188 (1990).
29. Reyes, A. *et al*. Target-cell-specific facilitation and depression in neocortical circuits. *Nature Neurosci.* **1,** 279–285 (1998).
30. Baude, A. *et al*. The metabotropic glutamate receptor (mGluR1 alpha) is concentrated at perisynaptic membrane of neuronal subpopulations as detected by immunogold reaction. *Neuron* **11,** 771–787 (1993).

Acknowledgements

We thank P. Cobden and P. Jays for assistance. This work was supported by the UK Medical Research Council (P.S.) and the NIH (C.E.J.).

Correspondence and requests for material should be addressed to D.E.B. (e-mail: berglesd@ohsu.edu).

Fringe forms a complex with Notch

Bong-Gun Ju*†, Sangyun Jeong*†, Eunkyung Bae*†‡, Seogang Hyun*§, Sean B. Carroll‖, Jeongbin Yim* & Jaeseob Kim*§

** National Creative Research Initiative Center for Genetic Reprogramming, Institute of Molecular Biology and Genetics, Seoul National University, Shinlim-Dong, Kwanak-Ku, Seoul 151-742, Korea*
‖ Howard Hughes Medical Institute and Laboratory of Molecular Biology, University of Wisconsin at Madison, 1525 Linden Drive, Madison, Wisconsin 53706, USA
§ Department of Biological Sciences, Korea Advanced Institute of Science & Technology, Kusong-dong, Yusong-ku, Taejon, 305-701, Korea
† These authors contributed equally to this work

The Fringe protein of *Drosophila* and its vertebrate homologues function in boundary determination during pattern formation[1–9]. Fringe has been proposed to inhibit Serrate–Notch signalling but to potentiate Delta–Notch signalling[10]. Here we show that Fringe and Notch form a complex through both the Lin–Notch repeats and the epidermal growth factor repeats 22–36 (EGF22–36) of Notch when they are co-expressed. The *Abruptex*^{59b}(*Ax*^{59b}) and *Ax*^{M1} mutations, which are caused by missense mutations in EGF repeats 24 and 25, respectively, abolish the Fringe–Notch interaction through EGF22-36, whereas the *l(1)N*^{B} mutation in the third Lin–Notch repeat of Notch abolishes the interaction through Lin–Notch repeats. *Ax* mutations also greatly affect the Notch response to ectopic Fringe *in vivo*. Results from *in vitro* protein mixing experiments and subcellular colocalization experiments indicate that the Fringe–Notch complex may form before their secretion. These findings explain how Fringe acts cell-autonomously to modulate the ligand preference of Notch and why the Fringe–Notch relationship is conserved between phyla and in the development of very diverse structures.

Fringe (Fng), an extracellular protein, determines the boundary of two different cell populations during the development of diverse

‡ Present address: Department of Ophthalmology & Visual Science, Catholic Research Institute of Medical Science, The Catholic University of Korea, Seocho-Gu, Seoul 137-701, Korea.